

GA-A22433

CONF-9608156--)

STABLE BOOTSTRAP-CURRENT DRIVEN EQUILIBRIA FOR LOW ASPECT RATIO TOKAMAKS

by

R.L. MILLER, Y.R. LIN-LIU, A.D. TURNBULL,
V.S. CHAN, L.D. PEARLSTEIN, O. SAUTER,
and L. VILLARD

RECEIVED

SEP 26 1996

OSTI

MASTER

AUGUST 1996

DISTRIBUTION OF THIS DOCUMENT IS UNLIMITED

 **GENERAL ATOMICS**

DISCLAIMER

This report was prepared as an account of work sponsored by an agency of the United States Government. Neither the United States Government nor any agency thereof, nor any of their employees, makes any warranty, express or implied, or assumes any legal liability or responsibility for the accuracy, completeness, or usefulness of any information, apparatus, product, or process disclosed, or represents that its use would not infringe privately owned rights. Reference herein to any specific commercial product, process, or service by trade name, trademark, manufacturer, or otherwise, does not necessarily constitute or imply its endorsement, recommendation, or favoring by the United States Government or any agency thereof. The views and opinions of authors expressed herein do not necessarily state or reflect those of the United States Government or any agency thereof.

STABLE BOOTSTRAP-CURRENT DRIVEN EQUILIBRIA FOR LOW ASPECT RATIO TOKAMAKS

by

R.L. MILLER, Y.R. LIN-LIU, A.D. TURNBULL,
V.S. CHAN, L.D. PEARLSTEIN,* O. SAUTER,**
and L. VILLARD**

This is a preprint of an invited paper presented at the ISPP
Workshop on Theory of Fusion Plasmas, August 26-31,
1996, Varenna, Italy, and to be printed in the *Proceedings*.

Work supported by U.S. Department of Energy
Grant DE-FG03-95ER54309 and Contract W-7405-ENG-48,
and in part by the Swiss National Science Foundation

*Lawrence Livermore National Laboratory
**CRPP/EPFL, Assoc. Euratom-Switzerland

GENERAL ATOMICS PROJECT 3726
AUGUST 1996

DISCLAIMER

Portions of this document may be illegible in electronic image products. Images are produced from the best available original document.

Stable Bootstrap-Current Driven Equilibria for Low Aspect Ratio Tokamaks

R.L. Miller, Y.R. Lin-Liu, A.D. Turnbull, V.S. Chan,
General Atomics, San Diego, California, U.S.A.

L.D. Pearlstein
Lawrence Livermore National Laboratory, Livermore, California, U.S.A

O. Sauter, L. Villard
CRPP/EPFL, Assoc. Euratom-Switzerland, Lausanne, Switzerland

Abstract

Low aspect ratio tokamaks can potentially provide a high ratio of plasma pressure to magnetic pressure β and high plasma current I at a modest size, ultimately leading to a high power density compact fusion power plant. For the concept to be economically feasible, bootstrap current must be a major component of the plasma current. A high value of the Troyon factor β_N and strong shaping are required to allow simultaneous operation at high β and high bootstrap current fraction. Ideal magnetohydrodynamic stability of a range of equilibria at aspect ratio 1.4 is systematically explored by varying the pressure profile and shape. The pressure and current profiles are constrained in such a way as to assure complete bootstrap current alignment. Both β_N and β are defined in terms of the vacuum toroidal field. Equilibria with $\beta_N \geq 8$ and $\beta \sim 35\%$ to 55% exist which are stable to $n = \infty$ ballooning modes, and stable to $n = 0, 1, 2, 3$ kink modes with a conducting wall. The dependence of β and β_N with respect to aspect ratio is also considered.

Low Aspect Ratio Tokamaks (LATs) have received significant attention recently in part because of the experimental results from START1 and the potential for tokamak operation at high plasma β , high plasma current, and modest size.² At low aspect ratio there is insufficient space on the inboard side of the tokamak for ohmic coils so non-inductive current drive for startup and current sustainment will be required. Additionally, the large plasma currents characteristic of low aspect ratio will require prohibitive amounts of non-inductive current drive power unless a large fraction of the current can be maintained by the bootstrap current. Thus we are led to study the magnetohydrodynamic (MHD) stability of the high β , large bootstrap fraction regime.

The high bootstrap fraction, $f_{bs} = I_{bootstrap}/I_p$ requirement — the equilibria here have f_{bs} in excess of 95% — constrains the current profile. Usually two independent plasma profiles determine an MHD equilibrium, *e.g.*, pressure and safety factor profiles. However, for high bootstrap fraction equilibria, the current profile is determined from the pressure profile alone; we use the collisionless model of Hirshman³ to model the bootstrap current. A small amount of auxiliary current is required near the axis where the bootstrap current goes to zero.

Although ultra-low aspect ratios have been proposed,² Stambaugh *et al.*⁴ show that given an assumed scaling of $\beta_N \propto 1/A$, the ratio of fusion power to Ohmic dissipation in the toroidal coil is maximized at $A = 1.4$. Although we present evidence that the scaling of β_N with A is weaker than $1/A$, suggesting larger optimal A than 1.4 with respect to this criterion, we primarily focus on $A = 1.4$ in this paper.

Some appreciation of the parameters required to achieve simultaneous high β and high bootstrap fraction can be seen from a simple relationship between β and β_p . The Troyon scaling for MHD stable β is given⁵

$$\beta = \frac{\beta_N}{100} \left(\frac{I}{aB} \right), \quad (1)$$

where I is in megamps, a is the minor radius in meters, B is in tesla, and β_N is in %-T-m/MA. At low A it is particularly important to identify the B used in this formula

and in the definition of β . We find that the above equation is best satisfied (*i.e.*, β_N nearly a constant) using the vacuum B field at the geometric axis of the outermost flux surface, B_0 . The plasma β is defined as the volume average of the pressure divided by the magnetic pressure due to this field

$$\beta = \frac{2\mu_0\langle p \rangle}{B_0^2} . \quad (2)$$

The poloidal β , β_p , is defined as the volume average of the pressure divided by the magnetic pressure due to an average poloidal field at the boundary

$$\beta_p = \frac{2\mu_0\langle p \rangle}{\bar{B}_p^2} = \frac{2\mu_0\langle p \rangle}{(\mu_0 I 10^6 / L_p)^2} \cong 25 \left(\frac{1 + \kappa^2}{2} \right) \frac{\beta_N}{100} \beta_N \left(\frac{aB_0}{I} \right) , \quad (3)$$

where we are still expressing I in megamps and use the approximation

$$L_p = 2\pi \sqrt{\frac{1 + \kappa^2}{2}} a , \quad (4)$$

for the poloidal circumference. Poloidal beta is a particularly important quantity in the present studies because the fraction of bootstrap current is proportional to β_p . Large f_{bs} will require large β_p . Multiplying Eq. (1) by Eq. (3) we get the desired result

$$\beta\beta_p = 25 \frac{1 + \kappa^2}{2} (\beta_N/100)^2 , \quad (5)$$

where β is now expressed as a number and not a percentage. This expression says that to achieve simultaneous high β and high bootstrap fraction (high β_p) we need high β_N and/or high elongation.

The numerical study presented here assesses the MHD stability of high β , low A equilibria for ideal infinite- n ballooning modes and low n kink modes. Additional details of some aspects may be found in Ref. 6. The low n stability analysis has been done only for selected cases, including the highest β cases. It appears, however, that for the beta range we study, the kink modes can be wall stabilized. Thus it is the ballooning mode which determines the β limit, while kink stability is determining the required wall location. We scan over a range of elongations and triangularities and find an optimal triangularity of

about 0.4 while β is still increasing with elongation up to the maximum κ we studied of 3. The optimum triangularity can be understood from the constraint on full bootstrap alignment at the edge.

The equilibria for this study were generated using the flux-coordinate fixed boundary code TOQ.⁷ This code can solve the Grad-Shafranov equation for a variety of different initial specifications. The code was recently modified and now uses a multigrid algorithm⁸ to invert the elliptic operator. In this paper we specify pressure and the flux surface average of $\langle J \cdot B \rangle$ where J is the plasma current and B is the magnetic field. $\langle J \cdot B \rangle$ near the plasma axis is assumed to result from auxiliary current drive while $\langle J \cdot B \rangle$ away from the axis is prescribed as a constant and is entirely generated from bootstrap current as described below. The formula for the pressure gradient, $p' \equiv \partial p / \partial \psi$, is specified as a function of normalized poloidal flux $\tilde{\psi}$, where $\tilde{\psi}$ varies from 0 at the magnetic axis to 1 at the boundary. A polynomial form found to be near optimal in this study is given by

$$p' = C(0.025 + 0.975 \tilde{\psi}^3 - \tilde{\psi}^4), \quad (6)$$

where the constant C is adjusted to give the desired β .

The primary contribution to $\langle J \cdot B \rangle$ is the bootstrap current. We use a simple model:

$$\langle J \cdot B \rangle_{\text{bootstrap}} = \mu_0 g(\tilde{\psi}) f p' , \quad (7)$$

based on the collisionless theory of Hirshman³ and described in more detail in Ref. 6. Here f is the flux function given by the major radius R times the toroidal field B_T , $f = RB_T$. We note in passing that the previously mentioned scaling $f_{\text{bs}} \propto \beta_p$ can be easily deduced from Eq. (7).

The infinite n ballooning mode equation was solved using BALOO⁷ and the low n kink modes were analyzed using GATO.⁹ The ballooning results were obtained by computing the marginal stable β for equilibria with resolutions of $(N_\psi, N_\theta) = [(67,65), (131,129), (259,257)]$ and extrapolating the results to the marginally stable β for infinite mesh size. Here N_ψ and N_θ are the number of radial and angular mesh points, respectively. Some of the equilibrium and ballooning results were reproduced using the

Lawrence Livermore National Laboratory code TEQ, while some low n kink results were confirmed using CHEASE¹⁰ and ERATO.¹¹

We first present equilibrium and stability results at $A = 1.4$ for a range of elongation, triangularity, temperature scale lengths, and p' profiles. All of the equilibria are marginally stable to ballooning modes. Kink analysis has been done for only a few representative cases, including the highest β cases. The case $\kappa = 3.0$, $\delta = 0.5$, and p' given by Eq. (6) is shown in Fig. 1. The pressure profile across the midplane as a function of major radius is shown in Fig. 1(b). The p' profile and q profiles as a function of $(\tilde{\psi})^{1/2}$ are shown in Fig. 1(c) and (d). The toroidal current density across the midplane as a function of major radius is shown in Fig. 2(a) and the peaking of the current density on the outboard midplane is quite striking. This is characteristic of LATs and is due to the strong variation of B with R . Note also that the q profile remains monotonic despite the off-axis peaking of the current density. The flux surface average $\langle JR_0 / R \rangle$ is shown in 2(b) to illustrate the total bootstrap alignment. The contributions to the "total bootstrap" current are shown individually as bootstrap, diamagnetic, and Pfirsch-Schluter contributions. The total bootstrap fraction for this equilibrium is 99% and the maximum stable β_N is 8.28. The β is 54% and β_p is 1.63. A wall at 1.3 times the plasma radius is sufficient to stabilize these modes.

The variation of maximum stable β_N and β with respect to triangularity δ and elongation κ are shown in Figs. 3 and 4. The Troyon factor β_N is seen to increase with increasing elongation but the increase in β is more dramatic because of the well-known increase in current I with elongation. β_p on the other hand is more nearly constant (Fig. 5) as a function of elongation and Eq. (5) shows in such a situation we expect β to increase as $(1 + \kappa^2)\beta_N^2$.

Somewhat surprisingly, Figs. 3 and 4 show a rather modest optimum triangularity. Ordinarily one would expect higher β with increasing triangularity from stability arguments. However, increasing triangularity also reduces the trapped particle fraction and thus the bootstrap current. This reduction in bootstrap current illustrated in Fig. 6 will increase the magnetic shear at the edge. Since in the equilibria considered here p' is required to vanish at the plasma boundary, the larger magnetic shear will make the transition from the second stability region to the first regime more difficult, hence, the

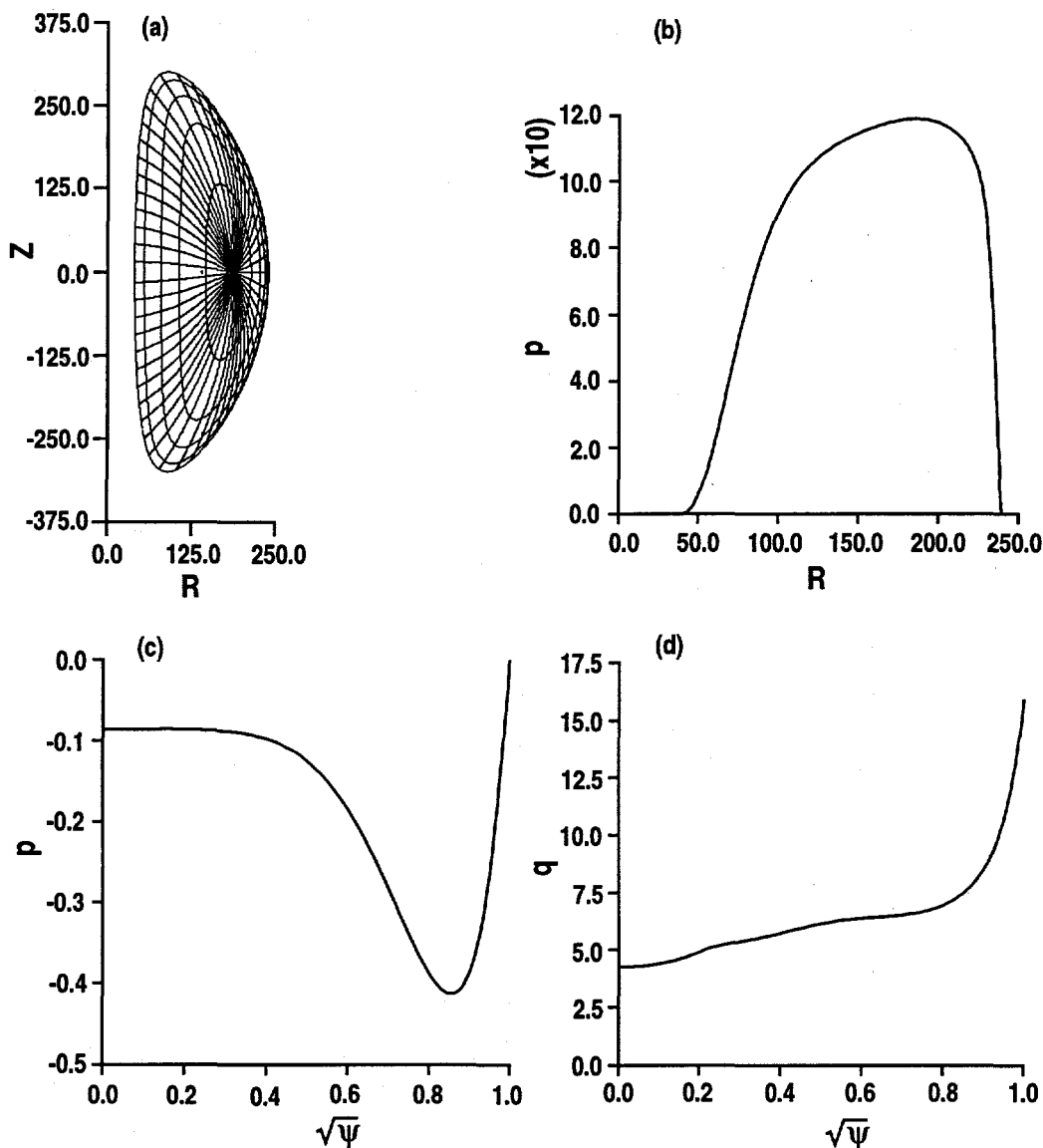


Fig. 1. Reference case equilibrium: $\kappa = 3.0$, $\delta = 0.5$, $L_p/L_T = 0.5$. (a) flux contours, (b) pressure profile across the midplane as a function of major radius, (c) p' as a function of $(\tilde{\psi})^{1/2}$, (d) q as a function of $(\tilde{\psi})^{1/2}$.

global β limit is lowered. There is a tradeoff in triangularity effects between increasing the magnetic well and increasing the magnetic shear. This results in an optimum triangularity which increases modestly with elongation (see Fig. 3). For $\kappa = 2.5$, $\delta = 0.3$ to 0.4. Although the optimum triangularity is near 0.4, wall stabilization becomes easier as δ

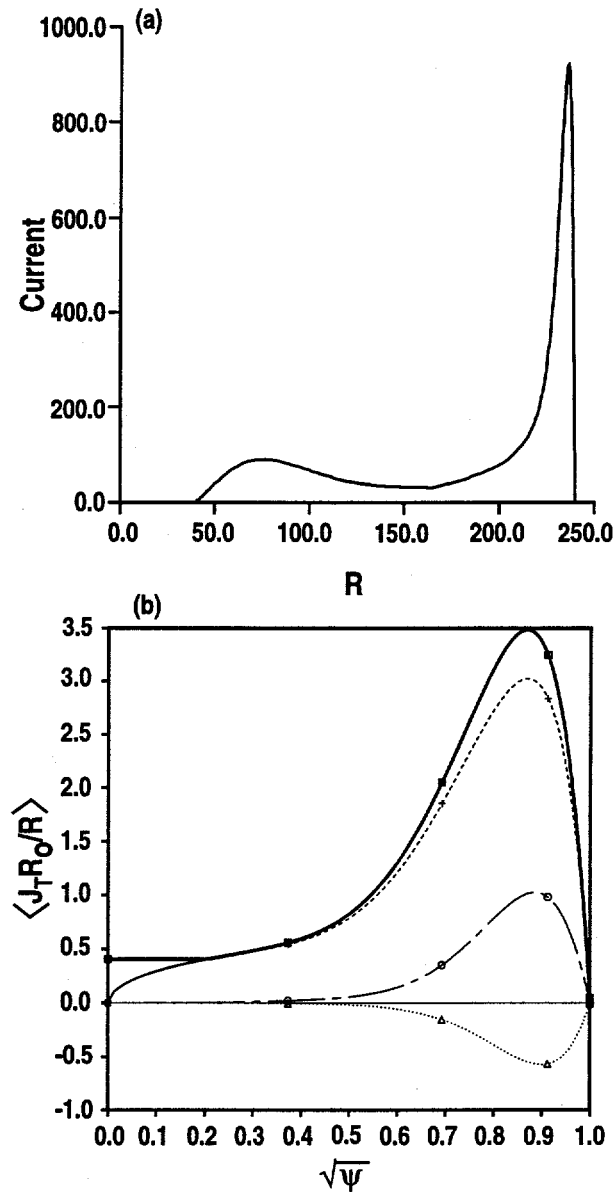


Fig. 2. Toroidal current density for equilibrium of Fig. 1. (a) toroidal current density across the midplane as a function of major radius and (b) $\langle J_{T0}/R \rangle$ versus $\sqrt{\psi}$. The components of the "total bootstrap" current density are shown individually as bootstrap (dash), diamagnetic (long dash, short dash), and Pfirsch-Schluter contributions (dots).

increases. For $\kappa = 3$, $r_{\text{wall}}/r_{\text{plasma}} = 1.15$ to stabilize $n = 1, 2$, and 3 at $\delta = 0.4$, while at $\delta = 0.5$, $r_{\text{wall}}/r_{\text{plasma}} \sim 1.3$. These wall locations are all adequate to stabilize the $n = 0$ mode for the respective equilibria.

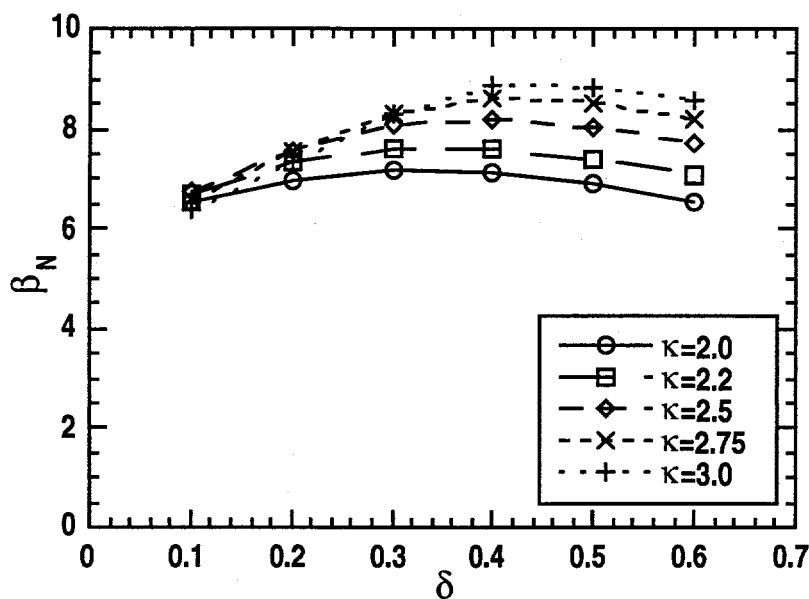


Fig. 3. Variation of β_N with respect to triangularity δ for a range of elongations.

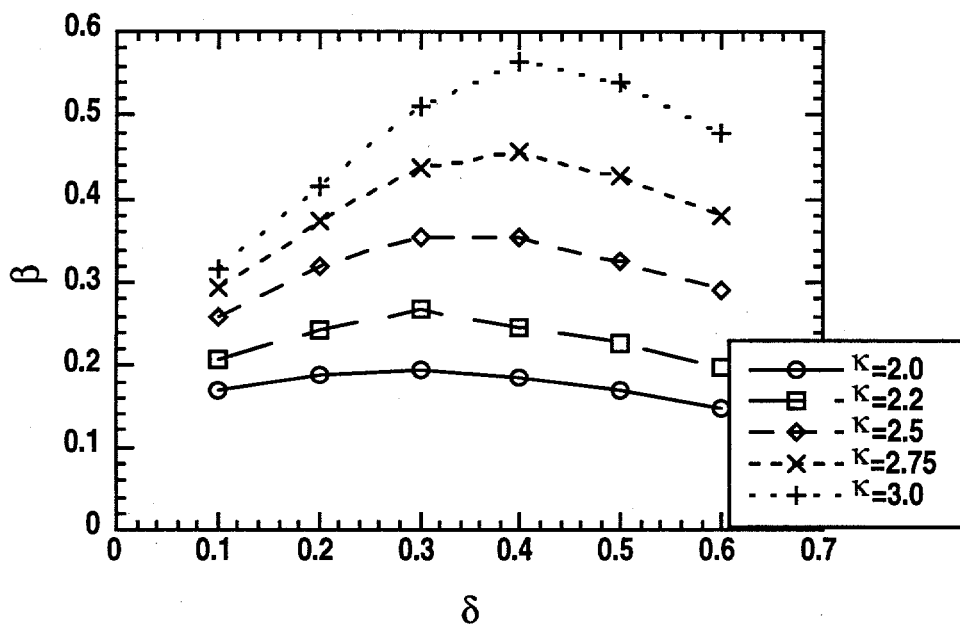


Fig. 4. Variation of β with respect to triangularity δ for a range of elongations.

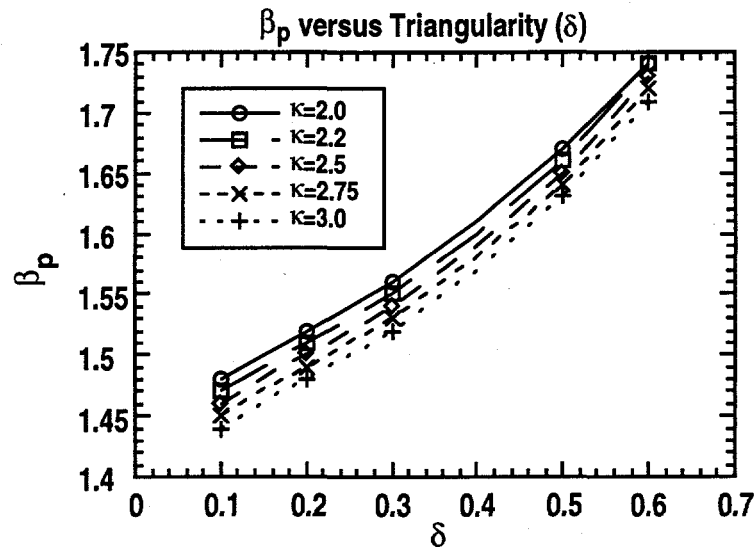


Fig. 5. β_p increases modestly with increasing triangularity. This increase is necessary to maintain constant $f_{bs} \sim 100\%$.

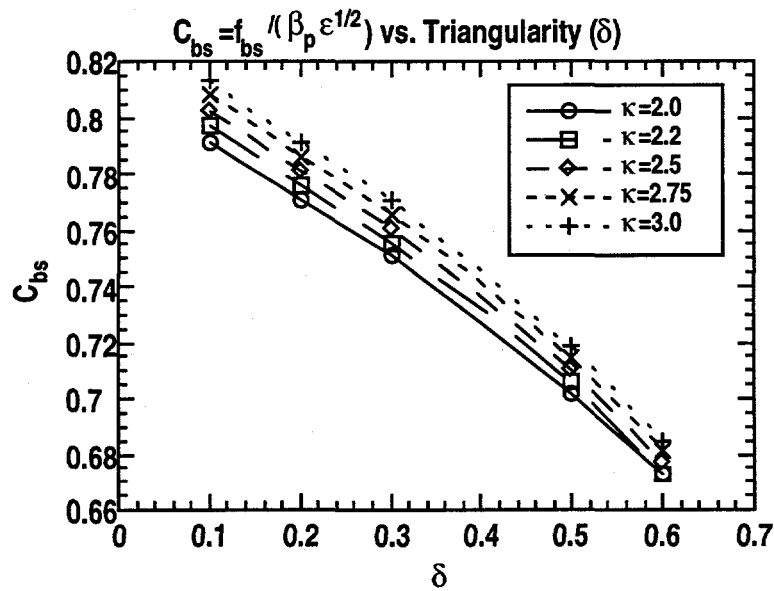


Fig. 6. The bootstrap coefficient $C_{bs} \equiv f_{bs} \sqrt{A}/\beta_p$ is seen to depend weakly upon elongation but decreases with triangularity. This higher β_p is required at larger δ to maintain f_{bs} .

As mentioned in the previous section, Eq. (6) for p' was found to be near optimal and Fig. 7 shows partial evidence for that. Here p' is parameterized as

$$p' = C(0.025 + 0.975 \tilde{\psi}^n - \tilde{\psi}^{n+1}),$$

and n is varied from 1 to 4. The maximum magnitude of p' occurs at $\tilde{\psi} = 0.975n/(n+1)$. The advantage of pushing the maximum towards the edge of the plasma is apparent from Fig. 7. The two different values of on-axis seed current in Fig. 7 show the advantage of raising q on axis. Note that $q_{\text{axis}} \propto 1/\langle J \cdot B \rangle_{\text{axis}}$. Further reductions of seed current beyond that shown produce almost no effect.

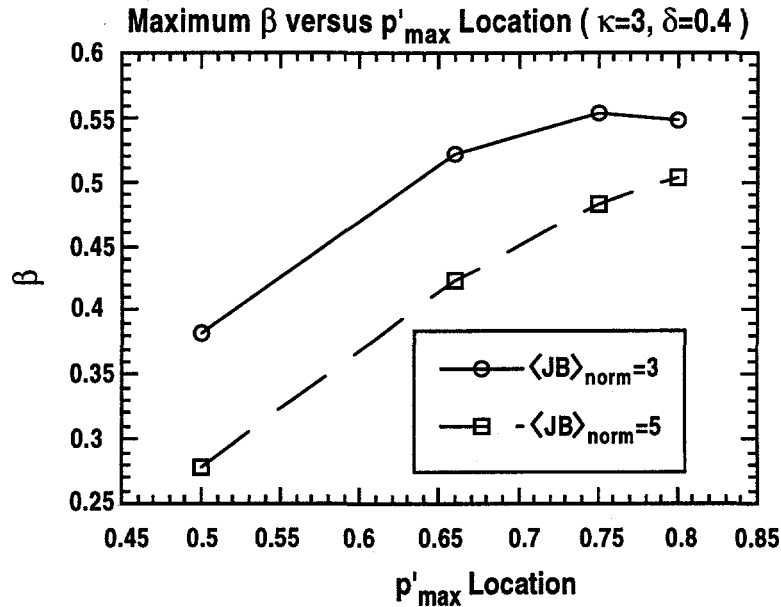


Fig. 7. Variation of β_N and β with respect to location of maximum p' for $\kappa = 3$ and $\delta = 0.4$. $\langle J \cdot B \rangle_{\text{norm}} \equiv \langle J \cdot B \rangle_{\text{axis}} a / B_0^2$.

It is also of interest to ask what limits the ballooning β to the values observed in this paper. This issue is addressed in Ref. 6 where $s - \alpha$ diagrams¹² are presented. It is shown that if p' is allowed to be finite at the edge of the plasma, as is routinely found in equilibrium reconstruction of DIII-D data,¹³ that $\beta_N \geq 10$ is possible. The equilibrium is in that case everywhere in the second stable regime.

Finally we consider the dependence of β and β_N upon aspect ratio. An attempt to study other A 's in as much detail as we have devoted to $A = 1.4$ would require extensive searches to determine an optimal $p'(\psi)$ at each A . We have taken the far more modest course of examining only ballooning stability and only for the p' profile given by Eq. (6) for A ranging from 1.2 to 2.8. We looked at a range of triangularities from 0.2 to 0.6 and at elongations of 2, 2.5, and 3. The results are shown in Figs. 8 and 9. Because we did not modify the profiles as we varied A , f_{bs} falls off somewhat for some of the higher A cases but is still always in excess of 80%. The triangularity yielding the highest β does not vary much at A . Even at $A = 2.8$ it is ~ 0.44 at $\kappa = 2$ and ~ 0.52 at $\kappa = 3$.

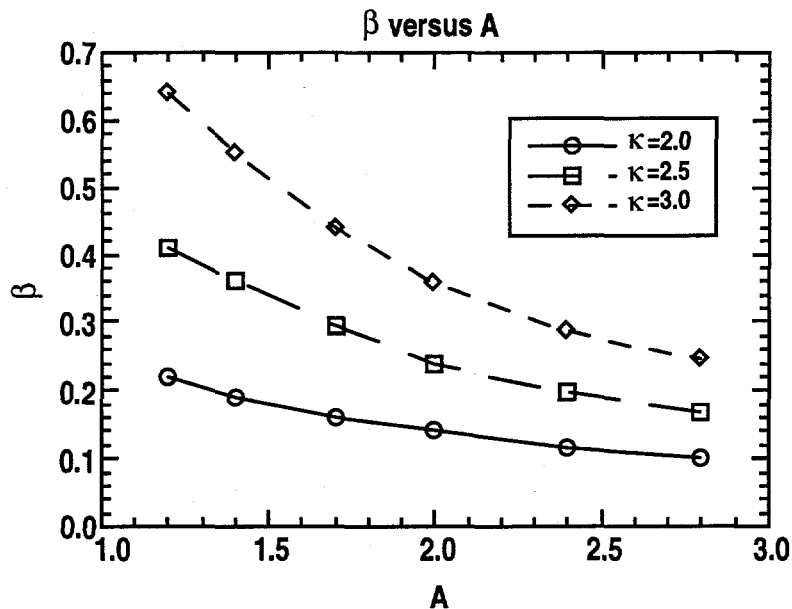


Fig. 8. Variations of β with respect to A for a range of elongations. Ballooning stability only.

Figures 8 and 9 show that higher elongation yields higher β and even higher β_N at every aspect ratio considered. The magnitude of $\beta_N \sim 6$ at $A = 2.8$ for $\kappa = 2$ is content

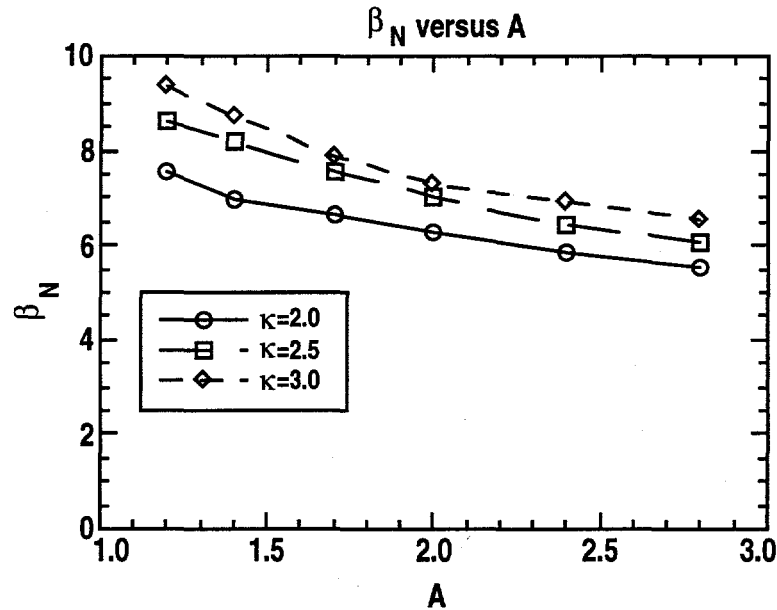


Fig. 9. Variations of β_N with respect to A for a range of elongations. Ballooning stability only.

with previous stability calculations¹⁴ in this parameter regime despite the large β_p 's (1.7 to 2 at $A = 2.8$) being considered here. Also the fact that $\beta_N(A = 1.2) > \beta_N(A = 1.4)$ even though p' was not optimized for $A = 1.2$ strongly suggests that β_N increases with decreasing A . Nevertheless, the reader is reminded of the limitations of this restricted optimization and, in particular, that wall stabilization of the kink at reasonable wall distances has not yet been demonstrated except at $A = 1.4$. In summary, we have explored the dependence of β and β_N on shape and pressure profile for the high β high bootstrap fraction tokamak regime at $A = 1.4$. We find with $f_{bs} \sim 99\%$ that ballooning mode instabilities limit β_N to the rather high range of ~ 8 with $p' = 0$ at the plasma edge. The cases examined for kink stability indicate that these modes can be wall-stabilized. The case with $\kappa = 3.0$ and $\delta = 0.5$ had $\beta = 55\%$. A triangularity of $\delta \sim 0.4$ is optimal while β increases significantly with elongation to the highest elongation studied ($\kappa = 3$).

This study is a step towards determining shapes and profiles at low aspect ratio to yield high β and high bootstrap fraction. Issues which remain to be addressed include: creating high β strongly shaped free-boundary equilibria with a realistic field-shaping coil

set, determining optimum pressure profiles consistent with a transport model, exploring effects of collisionality in the bootstrap current model, and assessing the need for current profile control.

This is a report of work sponsored by the U.S. Department of Energy under Grant No. DE-FG03-95ER54309 and Contract No. W-7405-ENG-48, and in part by the Swiss National Science Foundation.

References

1. A. Sykes, *Plasma Phys. and Contr. Fusion* **35**, 1051 (1993).
2. Y.-K.M. Peng *et al.*, in *Plasma Physics and Controlled Nuclear Fusion Research* (Proc. 15th Int. Conf. Seville, 1994) (International Atomic Energy Agency, Vienna, 1995) Vol. 2, p. 643.
3. S.P. Hirshman, *Phys. Fluids* **31**, 3150 (1988).
4. R.D. Stambaugh *et al.*, "The Spherical Tokamak Path to Fusion Power," General Atomics Report GA-A22226, to be submitted to Fusion Technology.
5. F. Troyon *et al.*, *Plasma Phys. and Contr. Fusion* **26**, 209 (1984).
6. R.L. Miller *et al.*, "Stable Equilibria for Bootstrap-Current Driven Low Aspect Ratio Tokamaks," General Atomics Report GA-A22321, submitted to Physics of Plasmas.
7. R.L. Miller and J.W. VanDam, *Nucl. Fusion* **28**, 2101 (1987).
8. P.M. de Zeeuw, Centre for Mathematics & Computer Science, P.O. Box 4079, 1009 AB Amsterdam, The Netherlands.
9. L.C. Bernard *et al.*, *Comput. Phys. Commun.* **24**, 377 (1981).
10. H. Lütjens, A. Bondeson, and A. Roy, *Comput. Phys. Commun.* **69**, 287 (1992).
11. R. Gruber *et al.*, *Comput. Phys. Commun.* **21**, 323 (1981).
12. J.M. Greene and M.S. Chance, *Nucl. Fusion* **21**, 453 (1981).
13. P. Gohil *et al.*, *Phys. Rev. Lett.* **61**, 1603 (1988); L.L. Lao *et al.*, *Plasma Phys. Contr. Fusion* **31**, 509 (1989).
14. W. Howl *et al.*, *Phys. Fluids B* **4**, 1724 (1992).